Int. J. Electrochem. Sci., 14 **(2019)** 7884 – 7898, doi: 10.20964/2019.08.74

International Journal of ELECTROCHEMICAL SCIENCE
www.electrochemsci.org

Medium Effect on the Electropolymerization and Electro-optical Properties of PEDOS

Kai Qu[§1], *Hongtao Liu*[§1], *Nannan Jian*[1], *Baoyang Lu*[2,*], *Ximei Liu*[2], *Jingkun Xu*[1,3,*]

[1] School of Chemistry & Chemical Engineering, Jiangxi Science & Technology Normal University, Nanchang 330013, Jiangxi, China
[2] School of Pharmacy, Jiangxi Science & Technology Normal University, Nanchang 330013, Jiangxi, China
[3] School of Chemistry and Molecular Engineering, Qingdao University of Science and Technology, Qingdao 266042, Shandong, China
[*]E-mail: lby1258@163.com and xujingkun1971@yeah.net
[§]These authors contributed equally to this work.

Received: 19 March 2019 / *Accepted:* 6 June 2019 / *Published:* 30 June 2019

3,4-Ethylenedioxyselenophene (EDOS), an important derivative of 3,4-ethylenedioxythiophene (EDOT), has better optoelectronic properties including lower band gap, better interchain charge transfer, lower oxidation and reduction potentials. In this work, the electropolymerization behavior of EDOS, and the electrochemistry, surface morphology, optical and electrochromic properties of the resultant PEDOS films are comparatively investigated in different solvent-electrolyte systems (CH_2Cl_2-Bu_4NPF_6, CH_2Cl_2-$BmimPF_6$, and pure $BmimPF_6$). We find that solvent-electrolyte systems exert influence on the electropolymerization behavior of EDOS monomer. EDOS displays lower onset oxidation potentials in CH_2Cl_2-$BmimPF_6$ and pure $BmimPF_6$ than commonly employed CH_2Cl_2-Bu_4NPF_6. PEDOS can be facilely electrodeposited in all these systems. Electrochromic results suggest that PEDOS film resulted from CH_2Cl_2-Bu_4NPF_6 medium exhibit relatively good transmittance changes ($\triangle$T%) of 26.5%, high coloration efficiency of 80 cm^2 C^{-1}. However, the addition of $BmimPF_6$ reveal a compact morphology, and enhanced the electrochemical stability and open circuit memory for PEDOS film. From these results, PEDOS can be further explored as electrochromic materials towards indoor electrochromic products and flexible displays.

Keywords: Conducting polymers, Electropolymerization, Electrochromics, 3,4-Ethylenedioxyselenophene, Medium Effect

1. INTRODUCTION

Owing to its excellent electrical, optical, electronic and electrochemical properties, poly(3,4-ethylenedioxythiophene) (PEDOT) and its derivatives as the most important conducting polymes (CP)

has attracted extensive attention on organic electronics like organic field effect transistors (OFETs), organic light-emitting diodes (OLEDs), electrochromic devices (ECDs), *etc*. The selenium analogue of PEDOT, poly(3,4-ethylenedioxyselenophene) (PEDOS), which was firstly synthesized by adopting a five-step synthetic methodology by Aqad et al.,[1] has better optoelectronic properties than PEDOT in some respects, such as lower band gap, enforced interchain charge transfer, lower oxidation and reduction potentials, and so on.[2-6] To further simplify the synthetic procedure hindering the extensive research of PEDOS, Patra *et al.* developed an efficient synthetic method to improve the research interest for PEDOS and its derivatives.[3] Currently PEDOS is mainly prepared by electrochemical polymerization, chemical oxidative polymerization and solid state polymerization. As a generally used synthetic strategy, electrochemical polymerization exhibits several unique advantages over other methods, including simple and easily controlled experimental conditions, one step poymerization with high reproducibility, easy device fabrication, etc.

Electrolytic medium has been demonstrated to exert significant impact on the electropolymerization behavior of the monomers and also the optoelectronic properties of the resultant polymers. Unfornately, such medium effect for the electropolymerization of EDOS and the corresponding PEDOS has not been systematically explored. High polarity and low nucleophilicity of solvents can increase the yield of polymer, owing to the reduction of coulomb repulsion during cationic coupling step.[7,8] Therefore, conventional organic solvents, dichloromethane (CH_2Cl_2),[9,10] propylene carbonate (PC)[11,12] and acetonitrile (CH_3CN),[13,14] are used in electrochemical polymerization frequently. Unfortunately, all these conventional organic solvents are mostly toxic, volatile and flammable. Two decades ago, room temperature ionic liquids (RTIL) were firstly applied to the electrosynthesis of conducting polymers.[15-18] Up to date, many conducting polymers including polyaniline, polypyrroles, polythiophenes, and so on [19-22], are successfully prepared by using ionic liquids owing to their wider electrochemical window, mild chemical conditions, ion mobility, lower volatility, lower toxicity, and so on. 1-Butyl-3-methylimidazolium hexafluorophosphate ($BmimPF_6$) is a common RTIL and has been employed for electrosynthesizing typical conducting polymers [19-22]. Some inherent shortcomings of such media such as high viscosity and poor solubility, can be readily overcome by the combination of RTIL and conventional solvents.[23] The introduced RTIL can act as both the solvent and electrolyte for the electropolymerization of EDOS and is expected to result in high-performance PEDOS films with less structural defects and improved properties.

Herein, we synthesize EDOS by a three-step synthetic procedure and systematically investigate the electropolymerization behavior of EDOS in different solvent-electrolytic systems including conventional solvent CH_2Cl_2-Bu_4NPF_6 (0.1 M), the binary system of CH_2Cl_2-$BmimPF_6$ (0.1 M) and pure RTIL $BmimPF_6$. Further, the medium effect on the polymerization and also the electro-optical performance of the resultant PEDOS film is camparatively discussed, including structural characterization, morphology, electrochemistry, and electrochromic performances of electrosynthesized PEDOS film from different media.

2. EXPERIMENTAL

2.1. Chemicals

2,3-Butanedione, (99%; Energy Chemical), trimethoxymethane, (99%; Energy Chemical), Methanol, (MeOH, analytical grade; J&K Chemical), H_2SO_4, (98%; Energy Chemical), selenium dichloride, ($SeCl_2$, 98%; J&K Chemical), Sodium acetate, (NaOAc, 98%; J&K Chemical), Hexane, (analytical grade; J&K Chemical), ethylene glycol, (99%; Energy Chemical), toluene, (99%; Energy Chemical), *p*-Toluenesulfonic acid (*p*-TSA, 99%; J&K Chemical), 1-butyl-3-methylimidazolium hexafluorophosphate ($BmimPF_6$, 99%; J&K Chemical) were all directly used as received Tetrabutylammonium hexafluorophosphate (Bu_4NPF_6, 99%; Energy Chemical) were dried under vacuum at 60 °C for 24 h before use. Dichloromethane (CH_2Cl_2, analytical grade; Beijing East Longshun Chemical Plant) was purified by distillation with calcium hydride, and stored with 4 Å molecular sieves prior to use. Other reagents were all analytical grade and used as received without further treatment.

2.2. Synthesis

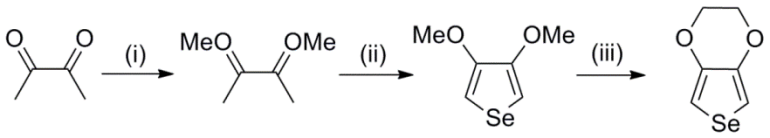

Figure 1. Synthetic route of EDOS monomer. Reagents and conditions: (i) trimethoxymethane, MeOH, H_2SO_4, 75 °C; (ii) $SeCl_2$, NaOAc, Hexane, -78 °C; (iii) ethylene glycol, *p*-TSA, toluene, 55 °C

2,3-Dimethoxy-1,3-butadiene [24], 3,4-dimethoxyselenophene and EDOS [3] were synthesized according to previously reported methods and their structures were confirmed by NMR, respectively. ^{1}H NMR (400 MHz, $CDCl_3$) for 2,3-dimethoxy-1,3-butadiene: δ 4.45 (d, 2H), 4.09 (d, 2H), 3.52 (s, 6H). ^{1}H NMR (400 MHz, $CDCl_3$) for 3,4-dimethoxyselenophene: δ 6.56 (s, 2H), 3.86 (s, 6H). NMR (400 MHz, $CDCl_3$) for 3,4-ethylenedioxyselenophene: ^{1}H NMR: δ 6.78 (s, 2H), 4.16 (s, 4H); ^{13}C NMR: δ 142.77, 101.55, 64.30.

2.3. Electrosynthesis and electrochemical tests

All solutions were deaerated with a dry nitrogen stream for 230 min, and the systems were maintained at a slight overpressure to avoid the effect of oxygen during the electrochemical experiments. A platinum disk electrode (3 mm in diameter, Wuhan GaossUnion Technology Co., Ltd., China) was employed as the working electrode. An Ag/AgCl electrode and a platinum wire (1 mm in diameter) were used as the reference and counter electrode, respectively. The areas of working and counter electrodes immersed into the electrolytic solution were calcualted to be 0.07 and 0.2 cm^2, respectively. A range of PEDOS films were electrochemically synthesized by using EDOS in CH_2Cl_2-

Bu_4NPF_6 (0.1 M) (yielding PEDOS[a]), CH_2Cl_2-$BmimPF_6$ (0.1 M) (yielding PEDOS[b]), and pure $BmimPF_6$ (yielding PEDOS[c]) systems in a one-compartment cell. The thickness of the PEDOS film was controlled by the total charge passed through the cell, which was read directly from the *I-t* curve by the computer. Anhydrous dichloromethane was used to repeatedly wash away the electrolyte and monomers/oligomers on the polymer films after the polymer film grew on the working electrode. Electrochemical tests of all these PEDOS films were carried out in monomer-free electrolyte solutions.

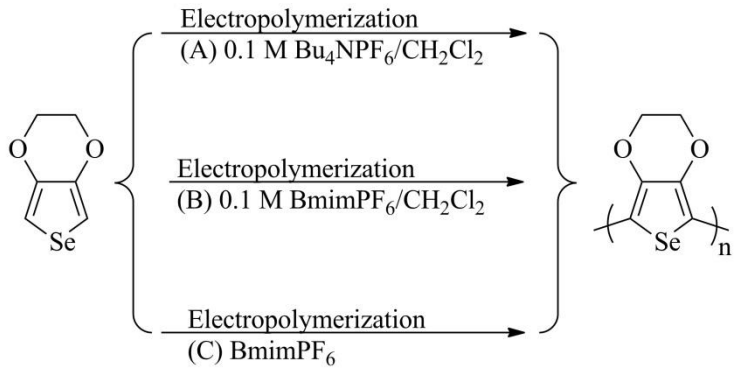

Figure 2. Schematic for the electropolymerization of EDOS in different solvent-electrolytic media.

To obtain a sufficient amount of the polymer films for other characterization, ITO-coated glass (3 × 2 cm^2) and Pt sheet (3 × 2 cm^2) were used as the working electrode and counter electrode, respectively.

2.4. Characterization

All the electropolymerization and electrochemical experiments were carried out with a VersaStat3 potentiostat/galvanostat (Princeton Applied Research). UV-vis spectra of both EDOS monomer and polymer were recorded on a SPECORD 200 PLUS UV-vis spectrophotometer. Fourier transform infrared (FTIR) spectra were characterized by using a Magna-IR 750 (American Nicolet Company) FT-IR spectrometer with samples in KBr pellets over the range from 4000 to 400 cm^{-1}. SEM images of different PEDOS films were taken on a Hitachi-S4800 scanning electron microscope with the polymer deposited on the ITO-coated glass.

The spectroelectrochemical studies of PEDOS films were carried out in a quartz cell with monomer-free electrolytes under the applied potential. The electrodes were an ITO-coated glass (working electrode), a Pt wire (counter electrode), and an Ag/AgCl (reference electrode), respectively. A blank ITO-coated glass in monomer-free electrolytes was used as the background in spectroelectrochemical measurements.

In a specific wavelength (λ_{max}), the optical density (ΔOD) and coloration efficiency (CE) can be determined by using the equations as listed below:[25,26]

$$\Delta OD = \log\left(\frac{T_{ox}}{T_{red}}\right) \quad (1)$$

$$CE = \frac{\Delta OD}{Q_d} \quad (2)$$

T_{ox} and T_{red} are the transmittance of the oxidized and reduced PEDOS films, respectively. Q_d is the injected/ejected charge.

3. RESULTS AND DISCUSSION

3.1 Electrochemical polymerization

Fig. 3 shows the anodic polarization curves of EDOS in different electrolytic media. The onset oxidation potential (E_{onset}) corresponds to the potentials that the monomers are oxidized to their radical cations, and lower E_{onset} can effectively reduce the occurrence of side reactions such as overoxidation and form higher quality polymer films.[20] E_{onset} of EDOS in CH_2Cl_2-Bu_4NPF_6, CH_2Cl_2-$BmimPF_6$ and pure $BmimPF_6$ are approximately at 1.10 V, 0.96 V and 0.98 V *vs* Ag/AgCl, respectively. Ionic liquid $BmimPF_6$ containing electrolytic media give EDOS lower E_{onset}, which would be beneficial for preparing high-quality PEDOS films.

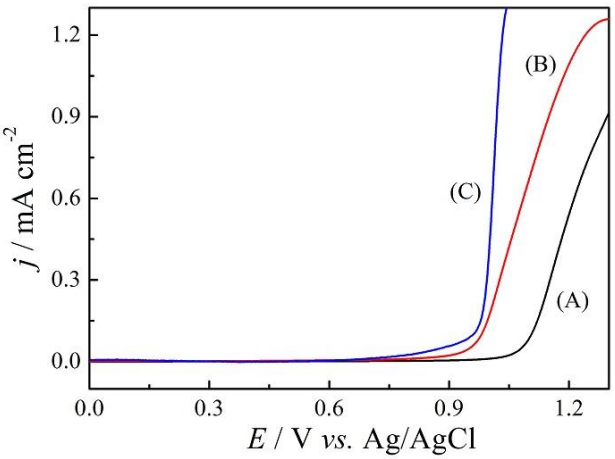

Figure 3. Anodic polarization curves of 0.1 M EDOS in (A) 0.1 M CH_2Cl_2-Bu_4NPF_6, (B) 0.1 M CH_2Cl_2-$BmimPF_6$ and (C) $BmimPF_6$, respectively. Potential scan rate: 20 mV s^{-1}.

Repetitive potential scanning of EDOS was recorded with potential intervals between -1.2 and 1.2 V in different media during the dynamic deposition process, as shown in Fig. 4.

Cyclic voltammetry (CV) curves recorded in all the three media (CH_2Cl_2-Bu_4NPF_6, CH_2Cl_2-$BmimPF_6$, and pure $BmimPF_6$) display prominent redox process with increasing current density at the potential range of -0.6 ~ 0.7 V. The oxidation and reduction peaks are first observed at around -0.2 ~ 0.2 V and then gradually shift towards higher potentials with further scanning.

Meanwhile, the CVs of EDOS electropolymerizatin in different solvent-electrolyte systems all show obvious and uniform peak currents increase along with continuous potential scanning, suggesting that the polymer films gradually form onto the electrode surface.[21] The broad redox wave of the depostied PEDOS films can be attributed to the broad distribution of the polymer chain length or the conversion of conductive species based on the PEDOS backbone from the neutral to oxidized states.

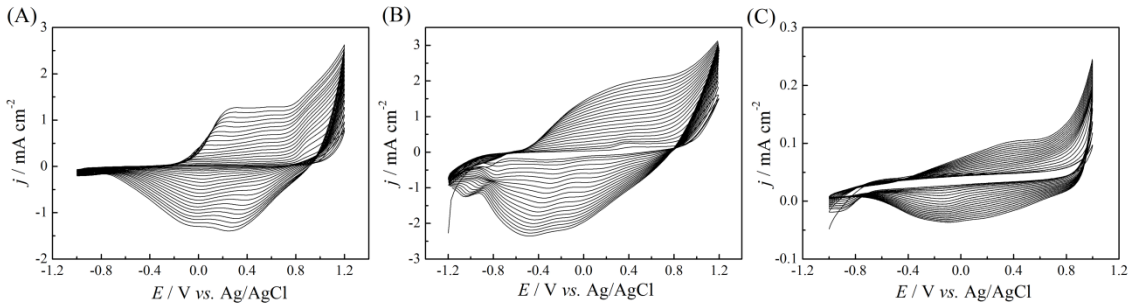

Figure 4. Cyclic voltammograms (CVs) of 0.1 M EDOS in CH_2Cl_2-Bu_4NPF_6 (0.1 M) (A), CH_2Cl_2-$BmimPF_6$ (0.1 M) (B) and pure $BmimPF_6$ (C). Potential scan rate: 20 mV s^{-1}.

The shift of anodic and cathodic peak potentials could be attributed to the fact that the increment of overpotential to overcome the electrical resistance increase of polymer film. This electrochemical behavior is characteristic of conductive polymers during the electrochemical deposition.

Additionally, the redox peak current densities of PEDOS in pure $BmimPF_6$ are lower than those in CH_2Cl_2-Bu_4NPF_6 and CH_2Cl_2-$BmimPF_6$ due to its high intrinsic viscosity (η = 275 mPa s at 25 °C measured in our lab) [27], which hinders the diffusion of EDOS from solution to the surface of the working electrode, thus the oligomeric species are not enough to form sufficient polymers on the working electrode. But the viscosities of CH_2Cl_2-Bu_4NPF_6 and CH_2Cl_2-$BmimPF_6$ are much lower than that of pure $BmimPF_6$, therefore the redox peak current densities are much higher.

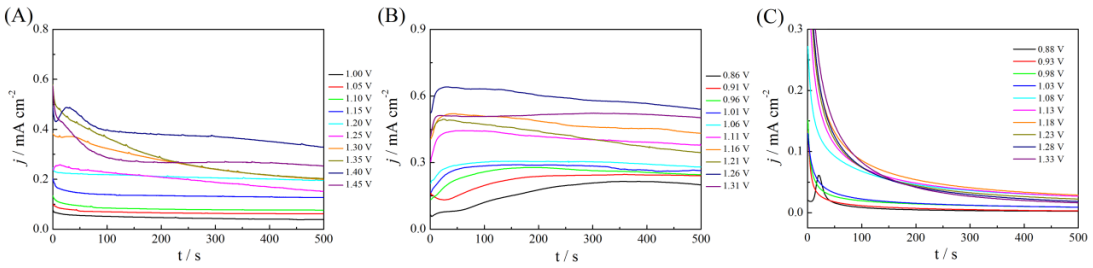

Figure 5. Chronoamperometry (constant potential polymerization) of 0.1 mol L^{-1} EDOS in 0.1 M CH_2Cl_2-Bu_4NPF_6 (A), 0.1 M CH_2Cl_2-$BmimPF_6$ (B) and pure $BmimPF_6$ (C) at different applied potentials as indicated for 500 s.

Different solvent-electrolyte systems could result in different qualities of the electrosynthesized PEDOS, thus it is important to optimize the polymerization potential to obtain high quality polymer films. *I-t* curves are recorded in different solvent-electrolyte systems under a series of applied

potentials higher than E_{onset}, as shown in Fig. 5 (0.1 M CH_2Cl_2-Bu_4NPF_6: from 1.0 to 1.45 V; 0.1 M CH_2Cl_2-$BmimPF_6$: from 0.86 to 1.31 V; $BmimPF_6$: from 0.88 to 1.33 V). Note here that no polymer was deposited on the working electrode until the applied potentials are higher than E_{onset}. Based on the experimental observation and *I-t* curves in Fig. 5, the optimized applied potentials for the electropolymerization of EDOS are demonstrated to be 1.30 V in CH_2Cl_2-Bu_4NPF_6, 1.16 V in CH_2Cl_2-$BmimPF_6$, and 1.18 V in pure $BmimPF_6$ (*vs* Ag/AgCl), respectively.

3.2. Structural characterization

FT-IR spectra are recorded to elucidate the structure of the PEDOS film and the polymerization mechanism of EDOS monomers, as shown in Fig. 6. The detailed peak assignments are summarized in Table 1. In comparison with EDOS, the absorption peaks of the polymers are broadened due to the wide chain dispersity of the dopsited polymers. The absorption at 3113 cm^{-1} can be assigned to the C-H stretching from the 2,5-position of the selenophene ring in EDOS, but it disappears in the FT-IR spectra of PEDOS electrosynthesized in all solvent-electrolyte systems,[28] suggesting that EDOS monomers are mainly electropolymerized through the coupling at the 2,5-position of the selenophene ring.

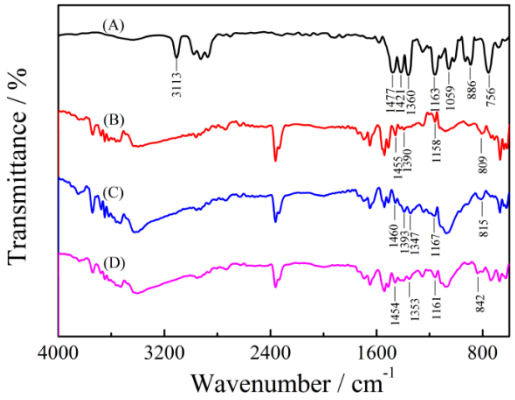

Figure 6. FT-IR spectra: EDOS (A), PEDOS obtained from 0.1 M CH_2Cl_2-Bu_4NPF_6 (B), 0.1 M CH_2Cl_2-$BmimPF_6$ (C), and pure $BmimPF_6$ (D) containing 0.1 M EDOS by constant potential electrolysis.

Table 1. Detailed peak assignments for the FT-IR spectra of EDOS and different PEDOS films.

Assignments and Notes	Wavenumber (cm^{-1})			
	EDOS	PEDOS[a]	PEDOS[b]	PEDOS[c]
C-H stretching at 2,5-position of the selenophene ring	3113	-	-	-
C=C and C-C stretching in the selenophene ring	1477 1421 1360	1455 1390	1460 1393 1347	1454 1353
C–O–C stretching vibrations in ethylene oxide unit	1163 1059	1158	1167	1161
C-Se stretching vibrations in selenophene ring	886 756	809	815	842

3.3. Morphology

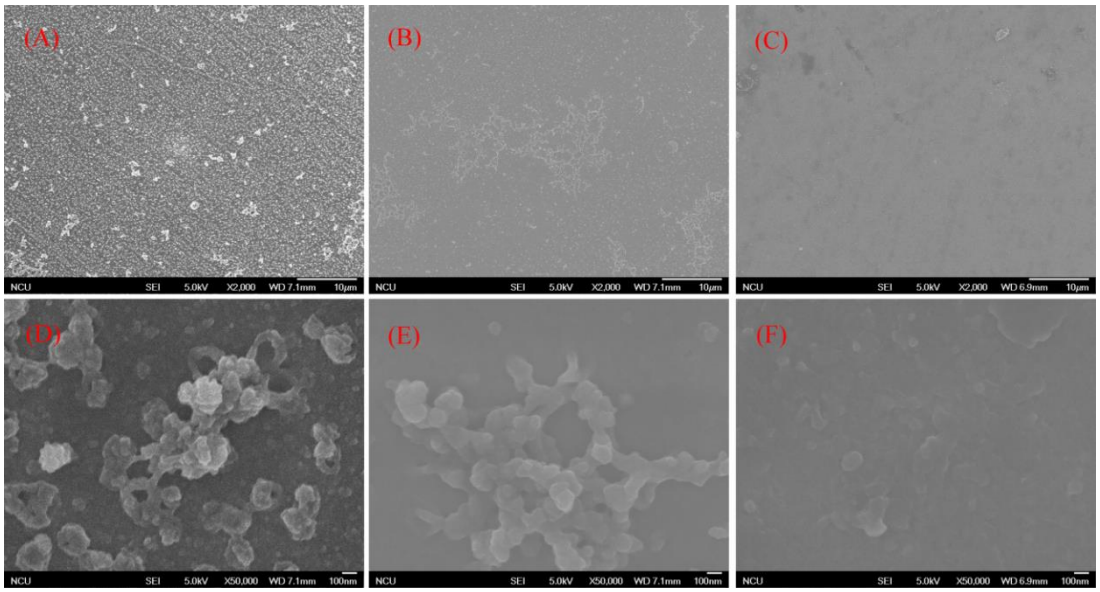

Figure 7. SEM of PEDOS films electrodeposited on the ITO-coated glass in three media: 0.1 M CH_2Cl_2-Bu_4NPF_6 (A and D), 0.1 M CH_2Cl_2-$BmimPF_6$ (B and E) and pure $BmimPF_6$ (C and F) containing 0.1 M EDOS.

Surface morphologies of PEDOS films electrosynthesized in different solvent-electrolyte systems are closely related to their optoelectronic properties. As can be seen from Fig. 7, PEDOS^a has a rough morphology with homogeneous distribution of particles, due to the fact that EDOS monomer and its radical cations can easily diffuse in CH_2Cl_2-Bu_4NPF_6 solution with low viscosity. In addition, the crystal nucleus of the oligomer particles could quickly form on the surface of electrode and the volume of the particles constantly increases as the polymerization process goes on. The morphology of PEDOS^b is smoother and the number of particles is less than PEDOS^a on the film surface, This is due to $BmimPF_6$ as the supporting electrolyte makes the viscosity of CH_2Cl_2-$BmimPF_6$ much higher than Bu_4NPF_6 in CH_2Cl_2 at 25 °C.[26]

The PEDOS^c presents a smooth and uniform morphology because of the high viscosity properties of $BmimPF_6$.[21] Compared with conventional organic solvents, the high viscosity of $BmimPF_6$ makes the EDOS monomer and its radical cations diffuse rather slowly and thus limits the polymerization rate of EDOS.[29,30] Therefore, the deposition rate of polymer film is slow. This mild chemical condition and limited deposition rate by $BmimPF_6$ result in smooth and compact surface morphology of PEDOS films on the electrode surface.

3.4. Electrochemistry of PEDOS

Fig. 8 shows the electrochemical behaviors of PEDOS, which are carried out in the corresponding monomer-free electrolyte systems. The detailed electrochemical parameters for electrosynthesized PEDOS films are presented in Table 2. During the scanning process, the cyclic voltammetry of the PEDOS films show significant hysteresis, and significant difference can be

observed between the anode and cathode peak potentials. The main reason is probably due to the following phenomena during ion diffusion or interface charge transfer: slow and inhomogeneous electron transfer, rearrangement between some polymer chains, and slow conversion of electron species.[31] In all these electrolytic systems, the good linear dependency between redox peak current densities and scan rates demonstrates that the redox process is non diffusional and PEDOS films are well-adhered to the working electrode.[32-33] The calculated $j_{p,a}$/ $j_{p,c}$ (the ratio between anodic or cathodic peak current density and potential scan rates) of PEDOS^{b} is closer to 1.0, much better than those of PEDOS^{a} and PEDOS^{c}, indicating the polymer has better redox reversibility.[34]

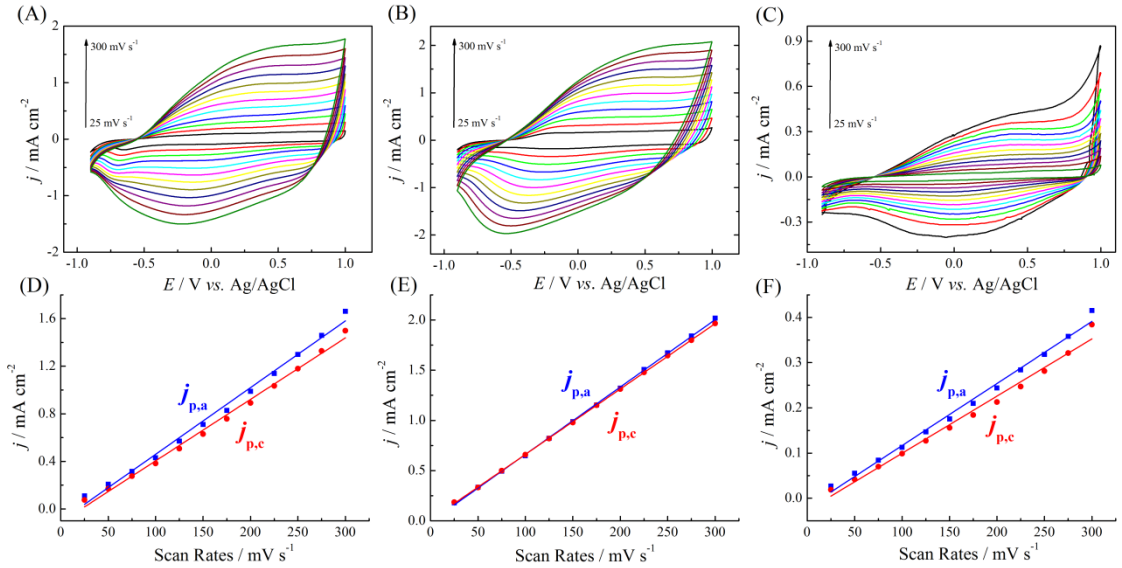

Figure 8. CVs of PEDOS films in monomer-free solvent-electrolyte systems: 0.1 M CH_2Cl_2-Bu_4NPF_6 (A), 0.1 M CH_2Cl_2-$BmimPF_6$ (B) and pure $BmimPF_6$ (C) at potential scan rates of 25, 50, 75, 100, 125, 150, 175, 200, 225, 250, 275, 300 mV s^{-1}. Plots of redox peak current densities *vs.* potential scan rates for different solvent-electrolyte systems: 0.1 M CH_2Cl_2-Bu_4NPF_6 (D), 0.1 M CH_2Cl_2-$BmimPF_6$ (E) and pure $BmimPF_6$ (F). j_p is the peak current density, and $j_{p,a}$ and $j_{p,c}$ denote the anodic and cathodic peak current densities, respectively.

Table 2. Electrochemical parameters for PEDOS tested in monomer-free electrolytic media.

Media	PEDOS				Ref.
	$E_{ox,peak}$ (V)	$E_{red,peak}$ (V)	R^2_{an}	R^2_{cat}	
Bu_4NPF_6 / CH_2Cl_2	0.60	-0.24	0.9925	0.9942	This work
$BmimPF_6$ / CH_2Cl_2	0.74	-0.57	0.9996	0.9999	This work
$BmimPF_6$	0.40	-0.06	0.9923	0.9867	This work
Microemulsion	-0.42	-0.56	0.988	0.991	[40]
ACN	0.41	-0.08	0.998	0.997	

3.5. Redox Stability

The redox stability of PEDOS films from different electrolytic media is investigated by long-term CVs, as shown in Fig. 9. After 100 cycles, the exchange charge of PEDOS[a] and PEDOS[b] maintain 18.5% and 33.2%, respectively. However, 37.9% for PEDOS[c] of it electrochemical activity is maintained after 1000 cycles. These results demonstrate that the employment of $BmimPF_6$ can improve the redox stability of PEDOS.

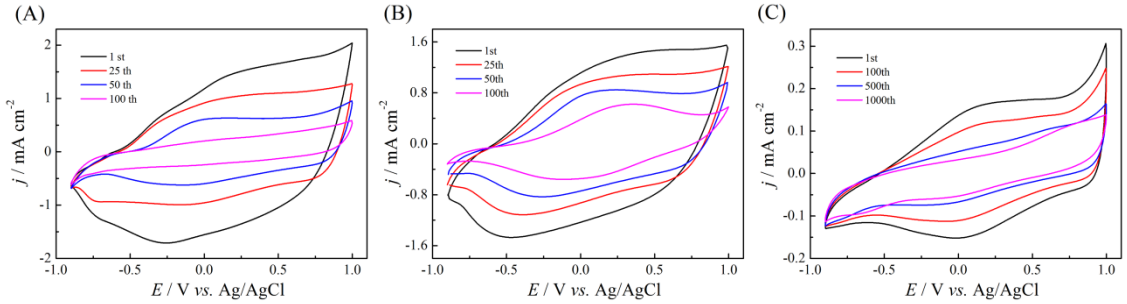

Figure 9. Long-term CVs of PEDOS films is deposited on Pt electrode in monomer-free solvent-electrolyte systems: 0.1 M CH_2Cl_2-Bu_4NPF_6 (A), 0.1 M CH_2Cl_2-$BmimPF_6$ (B) and pure $BmimPF_6$ (C) via cyclic scanning at the scan rate of 150 mV s^{-1}.

3.6. Spectroelectrochemistry

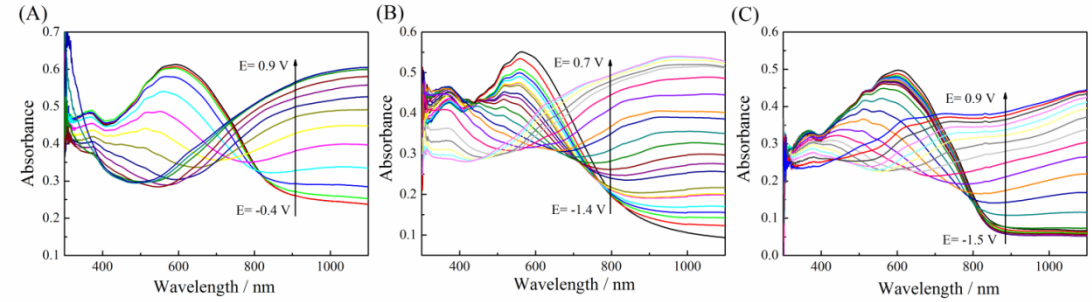

Figure 10. Spectroelectrochemistry of PEDOS films depostied on the ITO glass in 0.1 M CH_2Cl_2-Bu_4NPF_6 (A), 0.1 M CH_2Cl_2-$BmimPF_6$ (B) and pure $BmimPF_6$ (C) at different application potential ranges.

Spectroelectrochemical analyses are performed to examine the electrochromic properties of the resultant polymers in Fig. 10. Upon oxidation, the intensity of π–π* transition of PEDOS decreases and simultaneously a new band at longer wavelengths generates. The reason is probably that lower energy charge carriers (polarons and bipolarons) emerge during the oxidation process.[35] The band gap (E_g as shown in Table 3) is defined as the onset absorption of π–π* transition in the fully reduced polymer and it is generally obtained via the equation ($E_g = 1240/\lambda_{onset}$). The E_g of all the PEDOS films are calculated to be around 1.4 eV, in good agreement with the previous results measured in propylene carbonate.[3]

As compared with PEDOS[a] and PEDOS[b], the low-energy absorption peak of PEDOS[c] shifts to longer wavelength due to the short conjugated chain length.[35,36] The completely reduced PEDOS is gradually oxidized and the absorbance gradually decrease at the maximum absorbance peak (λ_{max}), because the electrons are removed from neutral PEDOS and the charge carriers (p-doping) are generated in the PEDOS film.

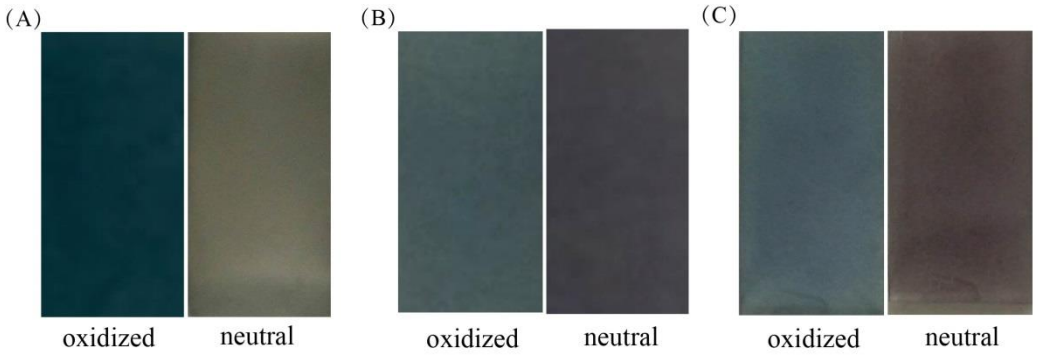

Figure 11. Color changing images of the PEDOS polymers from the oxidized state to the neutral state. PEDOS films were electrodeposited on the ITO-coated glass in 0.1 M CH_2Cl_2-Bu_4NPF_6 (A), 0.1 M CH_2Cl_2-$BmimPF_6$ (B) and pure $BmimPF_6$ (C) containing 0.1 M EDOS.

Table 3. Optical parameters of different PEDOS films.

Polymers	λ_{onset} (nm)	E_g (eV)	Colorimetric Results (CIE)			
			Applied potential	L	a	b
PEDOS[a]	855	1.45	-0.5 V	78.37	1.25	-2.17
			0.9 V	80.54	-0.42	-8.07
PEDOS[b]	874	1.41	-1.4 V	61.51	4.61	-8.93
			0.7 V	72.32	-3.60	-8.07
PEDOS[c]	845	1.47	-1.5 V	76.84	0.95	-7.65
			0.9 V	83.46	-1.53	-4.83

Overall, all fully oxidized PEDOS polymer films show similar color (blue) with visual observation. In the neutral state, the polymers reveal color changing phenomenon due to the absorption peaks appear at different wavelengths. Neutral PEDOS[a] and PEDOS[c] reveal a gray blue color, whreas the color of neutral PEDOS[c] is changed to purple as can be seen in Fig. 11. The electrons are delocalized along the conjugated backbones through the overlap of aromatic π-orbitals, which contributes to the π–π* transition.[37] The π–π* interband transition arises from an extended π-system with a filled narrow valence band and occur in the visible range, leading to a specific coloration.[38]

3.7. Electrochromic Performance

The electrochromic kinetic studies of PEDOS films are monitored by double-potential step chronoabsorptometry with different applied potentials at specific wavelengths (λ_{max} and 1050 nm). Fig. 12 and Table 4 summarize the electrochromic parameters of different PEDOS films. The potentials are

switched stepwise between the neutral and oxidative states with a residence time of 10 s. The optical contrast ratio of PEDOS[a] is found to be around 26.5%, superior to PEDOS[b] and PEDOS[c] at the corresponding λ_{max}. However, the PEDOS films show better optical contrast in the near-infrared region (1050 nm) than that in the visible region (the maximum optical contrast is 35.8% for PEDOS[b]).

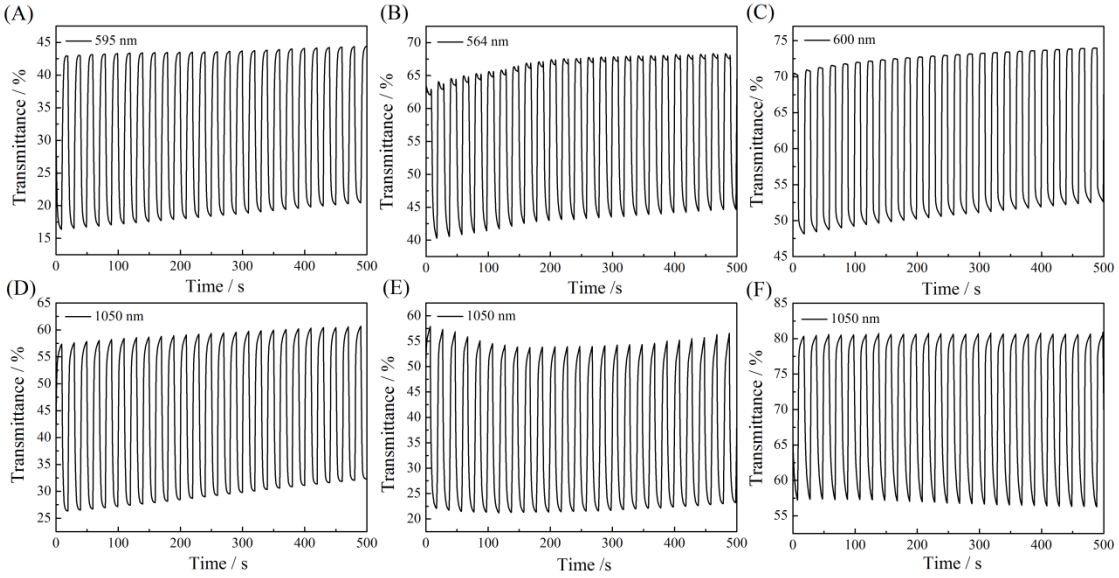

Figure 12. Electrochromic switching and optical absorbance are monitored for PEDOS films in 0.1 M CH_2Cl_2-Bu_4NPF_6 (A and D), 0.1 M CH_2Cl_2-$BmimPF_6$ (B and E) and pure $BmimPF_6$ (C and F).

Table 4. Comparison on the electrochromic performances for PEDOS, PEOTT, PEDOT in different solvent-electrolyte systems.

Polymers	Media	Wavelength (nm)	T_{neut} (%)	T_{ox} (%)	ΔT (%)	Response Time (s)		Coloration Efficiency ($cm^2\ C^{-1}$)	Ref.
						Oxidation	Reduction		
PEDOS[a]	CH_2Cl_2-Bu_4NPF_6	595	16.4	42.9	26.5	3.6	7.0	80	This work
		1050	57.4	26.3	31.1	4.3	5.2	27	
PEDOS[b]	CH_2Cl_2-$BmimPF_6$	564	40.3	63.7	23.4	2.3	6.0	29	This work
		1050	57.9	22.1	35.8	5.1	1.5	24	
PEDOS[c]	pure $BmimPF_6$	603	48.1	70.9	22.8	2.7	8.4	24	This work
		1050	80.4	57.3	23.1	7.4	4.8	44	
PEDOS	Microemulsion	600	26	31	5	7.10	8.00	24	[40]
	ACN	600	11	27	16	1.03	0.13	19	
PEOTT	CH_2Cl_2	600	10.7	46.9	36.2	1.2	1.3	182	[26]
		900	36.8	14.4	22.4	1.6	4.1	119	
	CH_2Cl_2-$BmimPF_6$	600	12.8	44.6	31.8	3.1	4.3	183	
		900	23.8	13.9	9.9	6.1	6.2	91	
	BmimPF6	600	30.3	8.0	22.3	3.1	6.4	212	
PEDOT	ACN	585	24.5	78.5	54.0	0.75	-	137	[41]

PEDOS[c] has a longer response time (achieving 95% of the full transmittance change) in comparison with those of PEDOS[a] and PEDOS[b], mainly because the high viscosity and poor fluidity of $BmimPF_6$ slow down the diffusing rate of counterions.[39]

PEDOS films are oxidized via forming cationic charges along with the polymer chains, and PF_6^- anions are inserted in the films to maintain electrical neutrality. The reduction process is oppositely accompanied by the release of counteranions. Coloration efficiency (CE) value is obtained from Equation (1) and (2) to evaluate the electrochromic performances of such PEDOS films, and the maximum CE value of PEDOS is about 80 cm^2 C^{-1} at 595 nm in CH_2Cl_2-Bu_4NPF_6.

3.8. Open circuit memory

The optical memory is important for the applications of electrochromic polymers, and it reflects the ability of color retention without applied voltages. As shown in Fig. 13, the transmittance curve is used to estimate the optical memory of different PEDOS films under the specifi wavelength of λ_{max}. Overall, the color of oxidized PEDOS film doesnot change obviously in the absence of applied voltage. However, the optical memory is significantly different in neutral state. In comparison with PEDOS^c, PEDOS^a and PEDOS^b show stronger optical constrast fluctuations of about 4.2% at -0.4 V and 4.5% at -1.4 V, respectively. This demonstrates that pure $BmimPF_6$ can minimize the self-erasing effect of PEDOS films.

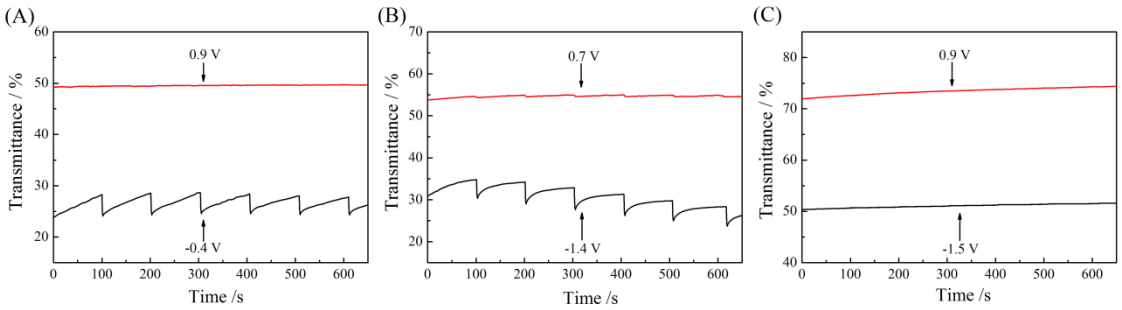

Figure 13. Open circuit memory of PEDOS monitored at 595 nm in 0.1 M CH_2Cl_2-Bu_4NPF_6 (A), 564 nm in 0.1 M CH_2Cl_2-$BmimPF_6$ (B) and 603 nm in pure $BmimPF_6$ (C). The potential is applied on PEDOS for 2 s and then potential-free for 100 s.

4. CONCLUSION

In this paper, EDOS, the selenium analog of EDOT, is electropolymerized in three different media, i. e., CH_2Cl_2-Bu_4NPF_6, CH_2Cl_2-$BmimPF_6$, and pure $BmimPF_6$. The medium effect on the electropolymerization of EDOS are studied though the detailed characterization on structure, electrochemical and electrochromic performance of as-formed PEDOS films. It is found that the mild chemical conditions and high intrinsic conductivity of $BmimPF_6$ decrease the onset oxidation potential of EDOS and produce a smooth and compact PEDOS film with improved redox stability. The combination of RTIL and conventional solvents (CH_2Cl_2-$BmimPF_6$) can also be a good medium, because EDOS can be effectively electropolymerized in CH_2Cl_2-$BmimPF_6$ with a relatively low onset oxidation potential (0.96 V). The PEDOS films show better optical contrast in the near-infrared region

(1050 nm) than that in the visible region, and the maximum optical contrast is demonstrated to be 35.8% for PEDOS prepared in CH_2Cl_2-$BmimPF_6$.

ACKNOWLEDGEMENTS

This work is supported by the National Natural Science Foundation of China (51763010, 51863009), Science Foundation for Excellent Youth Talents in Jiangxi Province (20162BCB23053), and the Key Research and Development Program of Jiangxi Province (20171BBH80007). J. X. thanks the financial support from the Innovation Driven "5511" Project of Jiangxi Province (20165BCB18016), and the Key Project of Natural Science Foundation in Jiangxi Province (20181ACB20010). X. L. thanks the Science and Technology Foundation of Jiangxi Educational Committee (GJJ160790). K. Q. thanks Jiangxi Educational Committee for a Postgraduate Innovation Program grant (YC2017-S409). N. J. thanks Jiangxi Science & Technology Normal University for a Postgraduate Innovation Program grant (YC2017X26).

References

1. E. Aqad, M.V. Lakshmikantham and M.P. Cava, *Org. Lett*., 3 (2001) 4283.
2. A. Patra, M. Bendikov and S. Chand, *Acc. Chem. Res*., 47 (2014) 1465.
3. A. Patra, Y.H. Wijsboom, S.S. Zade, M. Li, Y. Sheynin, G. Leitus and M. Bendikov, *J. Am. Chem. Soc.*, 130 (2008) 6734.
4. A. Patra and M. Bendikov*, J. Mater. Chem*., 20 (2010) 422.
5. S.S. Zade and M. Bendikov, *Org. Lett*., 8 (2006) 5243.
6. G.M. Nie, L. Wang and C.L. Liu, *J. Mater. Chem*. C., 3 (2015) 11318.
7. X.Y. Yang, C.L. Liu, J.B. Guo, L. Wang and G.M. Nie, *J. Polym. Sci., Part A: Polym. Chem*., 55 (2017) 2356.
8. W.Y. Yu, J. Chen, Y.L. Fu, J.K. Xu and G.M. Nie, *J. Electroanal. Chem*., 700 (2013) 17.
9. B.Y. Lu, S.J. Zhen, S.L. Ming and J.K. Xu, G.Q. Zhao*, RSC Advances*., 5 (2015) 70649.
10. B. Karabay, L.C. Pekel and A. Cihaner, *Macromolecules,* 48 (2015) 1352.
11. M. Li, A. Patra, Y. Sheynin and M. Bendikov, *Adv. Mater.*, 21 (2009) 1707.
12. M. Li, Y. Sheynin, A. Patra and M. Bendikov, *Chem. Mater*., 21 (2009) 2482.
13. Y.H. Wijsboom, A. Patra, S.S. Zade, Y. Sheynin, M. Li, L.J.W. Shimon and M. Bendikov, *Angew. Chem. Int. Ed.*, 121 (2009) 5551.
14. O. Dunand, T. Darmanin and F. Guittard, *ChemPhysChem*, 14 (2013) 2947.
15. S. Alkan, C.A. Cutler and J.R. Reynolds, *Adv. Funct. Mater.*, 13 (2003) 331.
16. X.B. Wan, F. Yan, S. Jin, X.R. Liu and G. Xue, *Chem. Mater*., 11 (1999) 2400.
17. C. Liu, J.X. Zhang, G.Q. Shi and Y.F. Zhao, *J. Phys. Chem*. B, 108 (2004) 2195.
18. F. Alakhras and R. Holze, *Synth. Met*., 157 (2007) 109.
19. B. Fan, L.T. Qu and G.Q. Shi, *J. Electroanal. Chem*., 575 (2005) 287.
20. F. Endres and S.Z. El Abedin, *Phys. Chem. Chem. Phys*., 8 (2006) 2101.
21. B. Dong, Y.H. Xing, J.K. Xu, L.Q. Zheng, J. Hou and F. Zhao, *Electrochim. Acta*, 53 (2008) 5745.
22. B. Dong, D.F. Song, L.Q. Zheng, J.K. Xu and N. Li, *J. Electroanal. Chem*., 633 (2009) 63.
23. Y.W. Zhu, S. Murali, M.D. Stoller, K.J. Ganesh, W.W. Cai, P.J. Ferreira, A. Pirkle, R.M. Wallace, K.A. Cychosz, M. Thommes, D. Su, E.A. Stach and R.S. Ruoff, *Science*, 332 (2011) 1537.
24. E. McDonald, A. Suksamrarn and R. D. Wylie, *J. Chem. Soc. Perk. T.*, 1 (1979) 1893.
25. C.L. Gaupp, D.M. Welsh, R.D. Rauh and J.R. Reynolds, *Chem. Mater*., 14 (2002) 3964.
26. B.D. Reeves, C.R.G. Grenier, A.A. Argun, A. Cirpan, T.D. McCarley and J.R. Reynolds, *Macromolecules*, 37 (2004) 7559.
27. Z.P. Wang, J.K. Xu, B.Y. Lu, S.M. Zhang, L.Q. Qin, D.Z. Mo and S.J. Zhen*, Langmuir*, 30 (2014)

15581.
28. B. Kim, J. Kim and E. Kim, Macromolecul*es*, 44 (2011) 8791.
29. P. Hapiot and C. Lagrost, *Chem. Rev*., 108 (2008) 2238.
30. K. Sekiguchi, M. Atobe and T. Fuchigami, *Electrochem. Commun*., 4 (2002) 881.
31. G. Inzelt, M. Pineri, J.W. Schultze and M.A. Vorotyntsev, *Electrochim. Acta*, 45 (2000) 2403.
32. T.A. Skotheim, R.L. Elsembaumer and J.R. Reynolds, CRC press, (1997).
33. J. Pringle, M. Forsyth, D. MacFarlane, K. Wagner, S. Hall and D. Officer, *Polymer*, 46 (2005) 2047.
34. Y.H. Wijsboom, Y. Sheynin, A. Patra, N. Zamoshchik, R. Vardimon, G. Leitus and M. Bendikov, *J. Mater. Chem.*, 21 (2011) 1368.
35. S.L. Ming, S.J. Zhen, K.W. Lin, L. Zhao, J.K. Xu and B.Y. Lu, *ACS Appl. Mater. Interfaces*, 7 (2015) 11089.
36. P. Camurlu, T. Duraka and L. Toppare, *J. Electroanal. Chem*., 661 (2011) 359.
37. S. Chen, B.Y. Lu, X.M. Duan and J.K. Xu, *J. Polym. Sci., Part A: Polym. Chem*., 50 (2012) 1967.
38. S. Duluard, B. Ouvrard, A. Celik-Cochet, G. Campet, U. Posset, G. Schottner and M.H. Delville, *J. Phys. Chem*. B, 114 (2010) 7445.
39. B.Y. Lu, S.M. Zhang, L.Q. Qin, S. Chen, S.J. Zhen and J.K. Xu, *Electrochim. Acta*, 106 (2013) 201.
40. W.N. Zhang, W.W. Zhang, H.T. Liu, N.N. Jian, K. Qu, S. Chen and J.K. Xu. *J. Electroanal. Chem*., 813 (2018) 109.
41. Z.P. Wang, D.Z. Mo, S. Chen, J.K. Xu, B.Y. Lu, Q.L. Jiang, Z.L. Feng, J.H. Xiong and S.J. Zhen, *J. Polym. Sci., Part A: Polym. Chem.*, 53 (2015) 2285.